

4

SECURITY

AD-A197 744

DTIC FILE COPY

RT DOCUMENTATION PAGE

1a. REPORT SECURITY CLASSIFICATION UNCLASSIFIED			1b. RESTRICTIVE MARKINGS		
2a. SECURITY CLASSIFICATION AUTHORITY			3. DISTRIBUTION / AVAILABILITY OF REPORT Approved for public release and sale. Distribution unlimited		
2b. DECLASSIFICATION / DOWNGRADING SCHEDULE			5. MONITORING ORGANIZATION REPORT NUMBER(S) <b>DTIC SELECTED</b> JUL 27 1988 H		
4. PERFORMING ORGANIZATION REPORT NUMBER(S) ONR Technical Report 19					
6a. NAME OF PERFORMING ORGANIZATION Department of Chemistry	6b. OFFICE SYMBOL (if applicable)	7a. NAME OF MONITORING ORGANIZATION			
6c. ADDRESS (City, State, and ZIP Code) State University of New York at Buffalo Buffalo, New York 14214		7b. ADDRESS (City, State, and ZIP Code)			
8a. NAME OF FUNDING / SPONSORING ORGANIZATION Office of Naval Research	8b. OFFICE SYMBOL (if applicable) ONR	9. PROCUREMENT INSTRUMENT IDENTIFICATION NUMBER N00014-84-K-0052			
8c. ADDRESS (City, State, and ZIP Code) Chemistry Program Arlington, Virginia 22217		10. SOURCE OF FUNDING NUMBERS			
		PROGRAM ELEMENT NO	PROJECT NO	TASK NO NR-051-855	WORK UNIT ACCESSION NO
11. TITLE (Include Security Classification) Corrosion Measurements using Microelectrodes					
12. PERSONAL AUTHOR(S) Kazimierz Wikiel and Janet Ostervang					
13a. TYPE OF REPORT Technical	13b. TIME COVERED FROM TO	14. DATE OF REPORT (Year, Month, Day) 1988 July 8		15. PAGE COUNT	
16. SUPPLEMENTARY NOTATION					
17. COSATI CODES			18. SUBJECT TERMS (Continue on reverse if necessary and identify by block number)		
FIELD	GROUP	SUB-GROUP	corrosion, microelectrodes, ohmic drop		
19. ABSTRACT (Continue on reverse if necessary and identify by block number) It is shown that microelectrodes can be substituted for large area electrodes in typical corrosion measurements. Results obtained for copper and iron in concentrated solutions are consistent with earlier literature reports. Application of microelectrodes markedly reduces effects of IR-ohmic drops. It allows one to apply electrochemical methods in corrosion investigations under conditions closer to those of natural corrosion environments. The corrosion rate of circular copper microelectrodes in 0.1 mol/dm <sup>3</sup> HCl solution depends on radius and increases with decreasing radius.					
20. DISTRIBUTION / AVAILABILITY OF ABSTRACT <input type="checkbox"/> UNCLASSIFIED/UNLIMITED <input checked="" type="checkbox"/> SAME AS RPT <input type="checkbox"/> DTIC USERS			21. ABSTRACT SECURITY CLASSIFICATION UNCLASSIFIED		
22a. NAME OF RESPONSIBLE INDIVIDUAL			22b. TELEPHONE (Include Area Code)	22c. OFFICE SYMBOL	

OFFICE OF NAVAL RESEARCH

Contract N00014-84-K-0052

Task No. NR 051-855

TECHNICAL REPORT NO. 19

Corrosion Measurements using Microelectrodes

by

Kazimierz Wikiel and Janet Osteryoung

Published in

Journal of Electrochemical Society

State University of New York at Buffalo  
Department of Chemistry  
Buffalo, New York 14214

July 1988

Reproduction in whole or in part is permitted for  
any purpose of the United States Government.

This document has been approved for public release  
and sale; its distribution is unlimited.

Corrosion Measurements Using Microelectrodes

Kazimierz Wikiel<sup>1</sup> and Janet Osteryoung

Department of Chemistry

State University of New York at Buffalo

Buffalo, New York 14214 (USA)


<sup>1</sup>Permanent Address: Institute of Precision Mechanics,

00-967 Warsaw, Duchnicka 3, Poland

# SUMMARY

It is shown that microelectrodes can be substituted for large area electrodes in typical corrosion measurements. Results obtained for copper and iron in concentrated solutions are consistent with earlier literature reports. Application of microelectrodes markedly reduces effects of IR-ohmic drops. It allows one to apply electrochemical methods in corrosion investigations under conditions closer to those of natural corrosion environments. The corrosion rate of circular copper microelectrodes in 0.1 mol dm<sup>-3</sup> HCl solution depends on radius and increases with decreasing radius.



Accession For	
NTIS GRA&I	<input checked="" type="checkbox"/>
DTIC TAB	<input type="checkbox"/>
Unannounced	<input type="checkbox"/>
Justification	
By	
Distribution/	
Availability Codes	
Dist	Avail and/or Special
A-1	

## INTRODUCTION

Unique features of very small, micrometer-size voltammetric electrodes cause the range of their application to be extended continuously. Microelectrodes have been used to solve neurophysiological problems both in vivo and in vitro [1-6]. Arrays of carbon fibers have been used as a voltammetric detector in high-performance liquid chromatography [7], whereas single ultramicroelectrodes have been applied in fast spectroelectrochemistry [8-10]. Microelectrodes have been used in electrochemical investigations in solvent without background electrolyte in order to reduce the effects of ohmic potential drops [11-16] or to extend the accessible potential range [17,18]. Microelectrodes have made it possible to make electrochemical measurements in such novel media as glass solvent eutectics [19] and the gas phase [20]. Micrometer size electrodes have been used in kinetics studies [21-23] and in investigations of nucleation of mercury at a microelectrode surface [22].

In this report we show that microelectrodes can be substituted for large area electrodes in typical corrosion measurements, and that the application of such small electrodes can give some novel advantages. The main advantage is that very high current densities can be achieved at low currents. Thus ohmic polarization can be made negligible even when the specific conductance of the solution is low. A second advantage is that at small electrodes steady state diffusional profiles are achieved at short times. Thus experiments can be carried out quickly. Finally, the dependence of the response on electrode radius, which is analogous to the dependence on rotation rate for a rotating disk, may prove useful in studies of localized corrosion processes such as pitting.

At an embedded circular electrode of radius  $r$  the limiting diffusion-controlled steady-state current for a simple charge transfer process is given by  $i_s = 4nFD Cr$ , where  $n$  is the number of electrons transferred,  $F$  the value of the Faraday, and  $D$  and  $C$  are the diffusion coefficient and bulk concentration, respectively, of reactant.

The steady-state current can be described using a diffusion layer model in which the thickness of the diffusion layer is  $\delta = \pi r/4$ . In contrast with the corresponding rotating disk case, the diffusion layer thickness does not depend on diffusion coefficient.

Here we describe results for two well-studied processes, the dissolution of iron and copper in deaerated chloride solutions.

## EXPERIMENTAL SECTION

Preparation of electrodes. To prepare circular copper electrodes, glass-coated 6  $\mu\text{m}$  (M. Fleischmann) and 10  $\mu\text{m}$ -diameter (Cu-99.99%, Goodfellow) copper wires were used. A piece of glass-coated wire approximately 3 cm long was sealed in vacuum into a 2- $\mu\text{L}$  glass micropipette (Drumond Scientific Co.) to confer mechanical stability and create a larger diameter insulating plane around the active electrode surface. This was done by inserting the glass-coated wire through the pipet, sealing one end, applying a vacuum, and then sealing a portion of the region under vacuum. The wire was then cut at this inner sealed position. This procedure prevented the copper from reacting chemically during the sealing process. In order to prepare the electrical connection, the inner glass coating from the copper wire was removed by using hydrofluoric acid. Then electrical connection was made with a silver thermosetting preparation (P-310 Johnson

Matthey Ltd.) and after that this part was covered with thermally shrinkable tubing. The cross section of copper sealed in glass was polished carefully by using a rotating wheel covered with a CarbiMet paper disk with decreasing grit size and subsequently with Microcloth polishing cloth with 1.0, 0.3 and 0.05- $\mu\text{m}$  alumina suspensions (Buehler Ltd.). The quality of the surface was checked optically with 500x magnification (Leitz-Dievert microscope). Only electrodes without any visible defects on the surface were taken for further experiments. Electrodes were repolished lightly before each experiment.

The preparation of circular iron electrodes (10- $\mu\text{m}$  diameter, glass coated, 99.99% Fe, Goodfellow) was carried out in a similar way. The initial seal between the glass-coated wire and the capillary was made with epoxy, because it was not possible to seal glass to glass directly in the presence of the reactive iron wire. In this case the inner glass coating was removed in molten sodium hydroxide. The resistance of electrodes was about 30, 10 and 70  $\Omega$  for 6- $\mu\text{m}$  Cu, 10- $\mu\text{m}$  Cu and 10- $\mu\text{m}$  Fe, respectively, and less than 1  $\Omega$  for electrodes with larger radii.

Instrumentation and chemicals. All experimental control, data collection and calculations were carried out on a DEC PDP 8/e laboratory minicomputer interfaced to an EG&G PARC model 273 potentiostat equipped with a Keithley model 427 current amplifier. The reference electrode was saturated calomel and all potentials are quoted with respect to this. A platinum counter electrode was used.

All reagents were of analytical grade, and distilled water passed through a Millipore Milli-Q purification system was used for preparation of the solutions. Solutions were purged with purified argon for at least 20 min. before each experiment. After purging, the argon was directed over the solution.

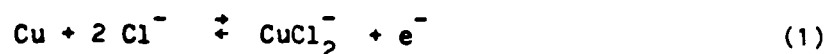
After a step-wise change in potential the steady-state value of current at an embedded circular electrode is achieved within 5% by time(s)  $6 \times 10^6 r^2$ , where  $r$  is in cm (assuming  $D = 9 \times 10^{-6} \text{ cm}^2/\text{s}$ ). In this work electrodes of  $r=3, 5, 12.5$ , and  $63.5 \times 10^{-4}$  cm were used. The corresponding times are 0.5, 1.4, 8.9, and 242 s, respectively. Experiments described here were carried out employing a staircase potential-time waveform with 2 mV step height and 2 s period. Thus all the data at the 6 and 10  $\mu\text{m}$ -diameter electrodes are obtained under diffusional steady state conditions, whereas for the 25- $\mu\text{m}$  electrode the first few points should exceed the steady state values. The very long times required to achieve steady-state diffusion at the 127- $\mu\text{m}$  electrode produce a different situation in which relaxation of concentration gradients is promoted by natural convection.

## RESULTS AND DISCUSSION

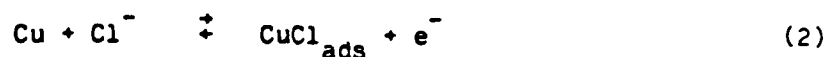
Typical anodic and cathodic polarization curves for a 25- $\mu\text{m}$  diameter copper electrode in deoxygenated  $0.1 \text{ mol dm}^{-3} \text{ HCl}$  solution are shown in Fig. 1. The cathodic Tafel plot has a slope of 120 mV/decade which is close to the values reported in the literature [24,25]. The anodic polarization curve consists of two regions and also agrees well with previous reports [25-30]. The first part is a straight line with slope about 60 mV/decade. The second part, occurring at potentials more positive than 0.0 V, has a higher slope. These two regions are separated by a region which displays some oscillations in the current.

The first part corresponds to the diffusion-controlled dissolution of Cu with the formation of  $\text{CuCl}_2^-$  as a final product, according to the overall equation:





According to Moreau [29,30] this reaction consists of three successive steps:



In this potential region the rate is governed entirely by diffusion on a uniform reaction surface. Braun and Nobe [28] have shown that diffusion of the chloride ions to the electrode surface is the rate-determining step under these conditions. For reaction (1) the Nernstian relation is

$$E = E_{1/2} - (1/f) \ln \{ 2(1 - i/i_d)^2 / (i/i_d) \}$$

$$E_{1/2} = E^\circ_{\text{Cu}^+/\text{Cu}} - (1/f) \ln \{ \beta_2 D_{\text{CuCl}_2} C_{\text{Cl}}^2 / 2 D_{\text{Cl}} \} \quad (5)$$

where  $i_d = 4FD_{\text{Cl}}C_{\text{Cl}}r$ ,  $f = F/RT$ , and  $\beta_2$  is the overall formation constant for  $\text{CuCl}_2^-$ . For small values of  $i/i_d$  the quantity  $(1 - i/i_d)^2$  may be approximated by unity. In fact the limiting current is not accessible experimentally, so in practice eq. (5) can only be applied when  $i/i_d$  is small. Rearranging we obtain

$$i = 4FD_{\text{CuCl}_2} C_{\text{Cl}}^2 \beta_2 r \exp \{ f(E - E^\circ_{\text{Cu}^+/\text{Cu}}) \} \quad (6)$$

Expressing this relation in terms of current density and steady-state diffusion layer thickness,  $\delta_s$ , we obtain

$$i/A = (FD_{\text{CuCl}_2} C_{\text{Cl}}^2 \beta_2 / \delta_s) \exp \{ f(E - E^\circ_{\text{Cu}^+/\text{Cu}}) \} \quad (7)$$

This expression is equivalent to that derived from the kinetic viewpoint by Smyrl [25]. In Figure 1, the maximum value of  $i/i_d$  is about 0.2, so eqn. (7) is a reasonable approximation which predicts the observed slope  $\partial \log i / \partial E = 60$  mV. We will return below to the question of dependence on concentration of chloride.

The steady-state voltammogram of Figure 2 shows more clearly the region of current oscillation. The details of the response here vary from experiment to experiment, but the general features are reproducible. Returning to Figure 1, the second part of the anodic copper dissolution curve, occurring beyond the region of current oscillations at more positive potentials, corresponds to transpassive dissolution of copper. Moreau [30], using X-ray diffraction methods, has identified two solid products at the copper surface,  $\text{CuCl}$  and  $\text{Cu}_2(\text{OH})_3\text{Cl}$ . Also Cooper and Bartlett [31] have observed formation of  $\text{Cu(II)}$  during anodic dissolution in this potential region. Up to 30% of the anodic current was attributed to formation of  $\text{Cu(II)}$ . Overshoots and oscillations at the beginning of this region (cf. Figure 2) were attributed to the formation and dissolution of a multilayer film on the electrode surface [31].

From the above it follows that results obtained at the circular copper microelectrode are in good agreement with the earlier data in the literature. Thus electrodes of small size are certainly appropriate for corrosion measurements. The small size also permits rapid measurements in the steady-state diffusional regime and thus reduces the amount of change in the surface during the course of the measurement. In the present case (Figure 1) with an effective potential scan rate of 1 mV/s, the amount of material lost in scanning from the corrosion potential to the passivation potential corresponds to about 0.3  $\mu\text{m}$  thickness of copper. Halving the scan rate would double that thickness.

The most important feature of the microelectrode is that the same valuable data available from large electrodes can be obtained by measuring very small total currents. At microelectrodes small currents give rise to relatively high current densities. This is shown in Figure 3, which

presents a Tafel plot for anodic dissolution of a smaller ( $10\text{-}\mu\text{m}$  diameter) circular iron electrode in  $1\text{ mol dm}^{-3}$  potassium chloride solution. Usually, even at such high concentrations of supporting electrolyte, anomalies in current-potential plots are observed very easily when conventional-size electrodes are used. These deviations are caused by ohmic  $iR$ -drops in the region of higher current densities, even if a Luggin probe is employed. In order to obtain plots of the proper shape, such techniques as positive feedback, current interruption, or some methods of calculations have to be used. This is unnecessary when microelectrodes with very small surface area are used instead of a conventional size electrode. For the microelectrode (Figure 3) a straight line log plot for anodic iron dissolution without any evidence of  $iR$  ohmic drops is observed up to  $0.2\text{ A/cm}^2$ , i.e. to the region where some effects connected to the transpassive dissolution of iron have been observed. Moreover a Luggin probe was not used in these experiments.

The anodic Tafel slope for electrodisolution of iron is about  $70\text{ mV/decade}$ , close to the value of  $80\text{ mV/decade}$  obtained by Asakura and Nobe [32] for the steady-state anodic polarization of iron in the same unbuffered neutral  $1\text{ mol dm}^{-3}$  KCl solution. However, their log plot was obtained by using the current interruption method. The apparent potential-log current relation deviated markedly from linearity for current densities above  $10\text{ mA/cm}^2$ .

Obviously, it is almost impossible to obtain a properly shaped potential-current relation at electrodes of "normal" size in solutions with markedly lower conductivity, even if sophisticated methods of ohmic  $iR$ -drop correction would be used. For instance, modern instrumentation such as the PARC 273 potentiostat allows one to compensate ohmic  $iR$  drops up to  $200\text{ }\Omega$  at the  $10\text{ mA}$  range or up to  $2\text{ M}\Omega$  at the  $1\text{ }\mu\text{A}$  range by using positive feedback.

Since the currents at microelectrodes reach the microampere level only in extreme conditions, ohmic  $iR$  drops due to high resistance can be corrected as needed. But this  $iR$  compensation is inadequate for even routine conditions at a large electrode.

Anodic dissolution curves for iron in  $10^{-4}$  mol  $\text{dm}^{-3}$  KCl solution are shown in Fig. 4. Resistivity of this solution is about  $60 \text{ k}\Omega \text{ cm}^{-1}$ . Curve A, obtained with a  $10 \text{ }\mu\text{m}$ -diameter circular electrode, is a straight line up to  $10 \text{ mA/cm}^2$ . Small deviations from linearity are observed above this limit. Curve B was obtained with a still small but markedly larger  $127\text{-}\mu\text{m}$  diameter iron electrode. No straight line region of the log plot can be identified in this case although the total currents are markedly lower than (less than one-thousandth of) those at electrodes used in typical corrosion measurements. (Note that the maximum current densities are no greater than about 1% of those expected for an anodic reaction diffusion-controlled in chloride.)

Since the use of microelectrodes reduces markedly ohmic  $iR$ -drops, it allows one to extend the range of corrosion measurements. As an example of such possibilities the anodic dissolution of copper over a wide range of chloride ions concentrations was chosen.

Anodic polarization curves of copper in chloride ion solutions with various concentration are shown in Fig. 5. A circular electrode with diameter of  $6 \text{ }\mu\text{m}$  was used. Concentrations of chloride ions are in the range  $1\text{-}10^{-4}$  mol  $\text{dm}^{-3}$ , and no other electrolytes were added to the solutions. Anodic behavior of copper depends markedly on concentration of chloride ion and can be divided into two regions. Above a concentration of  $0.01 \text{ mol dm}^{-3}$  log plots of anodic dissolution are straight lines and their slopes are approximately  $60 \text{ mV/decade}$ . According to Smyrl [25] for rotating disk

steady-state currents the anodic dissolution current density in this region can be described by:

$$1/A = (Fk_a D_{CuCl_2}^{1/2} C_{Cl}^2 / k_c \delta_L) \exp[(\alpha_a + \alpha_c)f(E-E^0)] \quad (8)$$

where  $k_a$  and  $\alpha_a$  are the anodic rate constant and charge transfer coefficient, respectively, and  $k_c$  and  $\alpha_c$  are the corresponding cathodic values. The quantity  $\delta_L$  is the Levich diffusion-layer thickness. The choice of reference potential makes  $k_a = k_c$ . Other symbols have their usual meanings. Assuming  $\alpha_a = \alpha_c = 0.5$  eq. (8) is equivalent to eq. (5) and the slope of a plot of  $E$  vs.  $\log i$  should be 60 mV/decade. From eq. (8) it follows that current density depends markedly on the concentration of chloride ions. Moreau [29] has investigated the effect of chloride ion concentration on anodic dissolution of copper within the range 0.1 to 10 mol  $dm^{-3}$ . He found the value of  $(dE/d \log C_{Cl})_{1,298} = 118$  mV. Our results obtained at copper microelectrodes are in good agreement with the theoretical prediction and with earlier reports. The log plot slopes of 60 mV/decade as well as the shift of the anodic curve 120 mV/decade  $C_{Cl}$  toward more positive potentials with decreasing chloride concentration down to 0.01 mol  $dm^{-3}$  are congruent with literature reports about anodic behavior of copper in solutions with higher chloride concentrations [28-30]. This means that even at chloride concentrations as low as 0.01 mol  $dm^{-3}$  the final product of anodic dissolution of copper is  $CuCl_2^-$ , and that diffusion is rate determining. Generally, in this region of chloride concentration the anodic dissolution of copper is governed by diffusion phenomena on a uniformly active surface.

At very low chloride ion concentration changes in shape of the current-potential curve are observed (Fig. 5, curves D,E). The slope of the log plots is 30-40 mV/decade at about 0.1  $mA/cm^2$ . It should be mentioned that

reproducibility of the results obtained with low chloride concentration is markedly poorer than in the higher range. The smaller slope probably reflects the same phenomenon as in the oscillation region in the solution with higher chloride concentration, i.e. the formation of multilayer films on the electrode surface. The second part of these curves indicate that transpassive oxidation of copper is involved in the electrodisolution process. It would be extraordinarily difficult to correct for iR drops under these conditions because the specific conductance of the solution changes markedly in the vicinity of the electrode during the course of the experiment [33].

Braun and Nobe [28] have estimated that in solution with chloride ion concentration lower than approximately  $0.05 \text{ mol dm}^{-3}$  a considerable amount of copper is dissolved as non-chloride-complexed copper(II) ions. The thermodynamic potential for equal concentrations of  $\text{Cu}^{2+}$  and  $\text{Cu}^+$  at the electrode surface is  $-0.082 \text{ V}$ , and  $\text{CuCl(s)}$  is thermodynamically stable only at more positive potentials. Taking into account only the species  $\text{Cu}^+$ ,  $\text{CuCl}_2^-$  and  $\text{Cu}^{2+}$ , the predominant species is  $\text{CuCl}_2^-$  except in  $10^{-3}$  and  $10^{-4} \text{ M Cl}^-$ . For these lower chloride concentrations  $\text{Cu}^+$  predominates except at higher current densities ( $> 0.6 \text{ mA/cm}^2$ ) where  $\text{Cu}^{2+}$  becomes increasingly important. Our results confirm the change of electrodisolution mechanism. However, also in the low chloride concentration range ( $1 \times 10^{-3} - 1 \times 10^{-4} \text{ mol dm}^{-3}$ ) a considerably smaller but still marked effect of chloride ion concentration on copper electrodisolution is observed.

Equation 5 predicts that the current density for copper dissolution should be inversely proportional to the diffusion layer thickness. The influence of diffusion layer thickness on anodic current density of copper in HCl solutions has been reported [25,28,29]. The thickness of the

diffusion layer has been changed by changing the rotation rate of a rotating disk electrode. Current densities were observed to increase as the rotation rate was increased. However, Braun and Nobe [28] have not observed direct proportionality to the square root of the rotation rate. Smyrl [25] has reported a closer fit to the expected dependence. Minor deviations have been observed at very high rotation rates. On the other side, Moreau [29] has reported a value of  $(dE/d \log \omega^{1/2})_{1,298} = -59 \text{ mV}$  which is in excellent agreement with eq. (5).

Since at microelectrodes the steady-state diffusion layer thickness is proportional to the electrode radius, anodic current density should be inversely proportional to the radius of a circular microelectrode. Typical curves of anodic dissolution of copper microdisk electrodes with different radii in  $0.1 \text{ mol dm}^{-3}$  hydrochloric acid are presented in Fig. 6. At the same potential value the anodic current density for smaller electrodes is larger than for larger ones. Since the cathodic process of hydrogen evolution does not depend on diffusion phenomena, the corrosion current density and corrosion potential obtained by extrapolation of straight parts of log plots to their intersection depend on the radius of the microelectrode. The corrosion current density is increased and corrosion potential is shifted toward more negative potentials with decrease in microelectrode radius.

An expression for the corrosion current can be obtained by equating the anodic current (eq. (8)) with the negative of the cathodic current (cf. Fig. 1). Assuming that all transfer coefficients are 0.5, we obtain

$$i_{\text{corr}} = k_{\text{CH}}^{2/3} (D_{\text{Cl}}^{1/2} C_{\text{Cl}}^{2/3})^{1/3} \quad (9)$$

where  $k_{\text{CH}}$  is the rate constant for hydrogen reduction at the corrosion potential. Using the value  $i^0 = 10^{-6.7} \text{ A/cm}^2$  for reduction of  $\text{H}^+$  on Cu

[24],  $k_{CH} = 10^{-11.7}$  cm/s. A plot of experimental corrosion current density vs  $r^{-1/3}$  for electrodes of radii 3, 5, and 12.5  $\mu\text{m}$  yielded a straight line with correlation coefficient 0.9998 and slope  $9.6 \times 10^{-9}$  A/cm<sup>5/3</sup>. The slope predicted by eq. (9) with  $D_{Cl} = 10^{-5}$  cm<sup>2</sup>/s is  $3.8 \times 10^{-9}$  A/cm<sup>5/3</sup>. Considering uncertainties in the data and in the appropriate value of  $k_{CH}$ , this is excellent agreement.

The same approach yields the prediction  $\partial V_{corr} / \partial \log r = 40$  mV. A plot of  $E_{corr}$  vs  $\log r$  was linear (correlation coefficient = 0.9996) with slope 26 mV. Thus the shift in corrosion potential is less than predicted.

A final comment on the use of microelectrodes for studying corrosion processes concerns the role of geometry in the formation of single pits. Beck and Alkire have discussed the role of spherical diffusion in formation of pits [34]. The relation confirmed here between size and corrosion rate for a homogeneous surface demonstrates experimentally the prediction of higher corrosion rates at small sites on a heterogeneous surface. Furthermore, it seems feasible to study small electrodes under conditions where only one pit can form and thus to examine more quantitatively models which describe this process, especially in its early stages.

#### ACKNOWLEDGMENTS

This work was supported in part by the Office of Naval Research. The 6- $\mu\text{m}$  diameter copper wires were supplied by Martin Fleischmann, University of Southampton, Southampton, England.



## REFERENCES

1. L. C. Clark, C. Lyons: *Ala. J. Med. Sic.*, 2(4), (1965), 355.
2. R. N. Adams: *Anal. Chem.*, 48, (1976), 1126A.
3. J. L. Ponchon, R. Cespuglio, F. Gonon, M. Jouvet, J. F. Pujol: *Anal. Chem.*, 51, (1979), 1483.
4. M. A. Dayton, J. C. Brown, K. J. Stutts and R. M. Wightman: *Anal. Chem.*, 52, (1980), 945.
5. M. A. Dayton, A. G. Ewing and R. M. Wightman: *Anal. Chem.*, 52, (1980), 2392.
6. A. G. Ewing, M. A. Dayton and R. M. Wightman: *Anal. Chem.*, 53, (1981), 1942.
7. R. M. Wightman, W. L. Candill, J. O. Howell: *Anal. Chem.*, 54, (1982), 2532.
8. R. S. Robinson and R. L. McCreery: *Anal. Chem.*, 53, (1981), 997.
9. R. S. Robinson, C. W. McCurdy and R. L. McCreery: *Anal. Chem.*, 54, (1982), 2356.
10. R. S. Robinson and R. L. McCreery: *J. Electroanal. Chem.*, 182, (1985), 61.
11. R. Lines and V. D. Parker: *Acta Chem. Scand.*, B31, (1977), 369.
12. J. O. Howell and R. M. Wightman: *J. Phys. Chem.*, 88, (1984), 3915.
13. A. M. Bond, M. Fleischmann and J. Robinson: *J. Electroanal. Chem.*, 168, (1984), 299.
14. A. M. Bond, M. Fleischmann and J. Robinson: *J. Electroanal. Chem.*, 172, (1984), 11.
15. A. M. Bond, P. A. Lay: *J. Electroanal. Chem.*, 199, (1986), 285.

16. M. J. Pena, M. Fleischmann and N. Garrard: J. Electroanal. Chem., 220, (1987), 31.
17. J. Cassidy, S. P. Khoo, S. Pons and M. Fleischmann: J. Phys. Chem., 89, (1985), 3933.
18. T. Dibble, S. Bandyopadhyay, J. Ghoroghchian, J. J. Smith, F. Sarfarazi, M. Fleischmann and S. Pons: J. Phys. Chem., 90, (1986), 5275.
19. A. M. Bond, M. Fleischmann and J. Robinson: J. Electroanal. Chem., 180, (1984), 257.
20. J. Ghoroghchian, F. Safarazi, T. Dibble, J. Cassidy, J. J. Smith, A. Russell, G. Dunmore, M. Fleischmann and S. Pons: Anal. Chem., 58, (1986), 2278.
21. J. O. Howell, R. M. Wightman: Anal. Chem., 56, (1984), 524.
22. B. Schafiker, G. J. Hills: J. Electroanal. Chem., 130, (1981), 81.
23. Z. Galus, J. Golas and J. Osteryoung:
24. J. O'M. Bockris and N. Pentland: Trans Faraday Soc., 48, (1952), 833.
25. W. H. Smyrl: in Comprehensive Treatise of Electrochemistry, Vol. 4; p. 97-149, (eds. J.O'M. Bockris, B. E. Conway, E. Yeager, R. E. White), Plenum Press, NY 1981.
26. B. Miller and M. J. Bellavance; J. Electrochem. Soc., 119, (1972), 1510.
27. A. L. Baccarella and J. C. Griess: J. Electrochem. Soc., 120, (1973), 459.
28. M. Braun and K. Nobe: J. Electrochem. Soc., 126, (1979), 1666.
29. A. Moreau: Electrochim. Acta, 26, (1981), 497.
30. A. Moreau: Electrochim. Acta, 26, (1981), 1609.

31. R. S. Cooper and J. H. Bartlett: J. Electrochem. Soc., 105, (1958), 109.
32. S. Asakura and K. Nobe: J. Electrochem. Soc., 118, (1971), 13.
33. M. G. Athayde, O. R. Mattos, and L. Sathler, Electrochim. Acta, 32, (1987), 909-913.
34. T. R. Beck and R. C. Alkire: J. Electrochem. Soc., 126, (1979), 1662-1666.

## FIGURE LEGENDS

Figure 1. Anodic and cathodic polarization of copper in  $0.1 \text{ mol dm}^{-3} \text{ HCl}$  solution. Circular copper electrode, diameter  $25 \text{ }\mu\text{m}$ ; staircase voltammetry:  $t = 2\text{s}$ ;  $\Delta E_s = 2\text{mV}$ .

Figure 2. Anodic staircase voltammogram of copper in  $0.1 \text{ mol dm}^{-3} \text{ HCl}$ . Circular copper electrode, diameter  $10 \text{ }\mu\text{m}$ ;  $t = 2\text{s}$ ;  $\Delta E_s = 2 \text{ mV}$ .

Figure 3. Anodic polarization of iron in  $1 \text{ mol dm}^{-3} \text{ KCl}$  solution. Iron microdisk,  $10 \text{ }\mu\text{m}$  in diameter. Staircase voltammetry:  $t = 2\text{s}$ ;  $\Delta E_s = 2\text{mV}$ .

Figure 4. Anodic polarization of iron in  $1 \times 10^{-4} \text{ mol dm}^{-3} \text{ KCl}$  solution. Iron disk: A- $10 \text{ }\mu\text{m}$ ; B- $127 \text{ }\mu\text{m}$  in diameter. Staircase voltammetry:  $t = 2\text{s}$ ;  $\Delta E_s = 2\text{mV}$ .

Figure 5. Anodic polarization of copper in chloride solutions:  $1 \times 10^{-4} \text{ mol dm}^{-3} \text{ HCl}$  +: A- 0.9999 ; B- 0.0999 ; C- 0.0099 ; D- 0.0009 ; E- 0.0000  $\text{mol dm}^{-3} \text{ KCl}$ . Copper microdisk,  $6 \text{ }\mu\text{m}$  in diameter. Staircase voltammetry:  $t = 2\text{s}$ ;  $\Delta E_s = 2\text{mV}$ .

Figure 6. Anodic polarization of copper in  $0.1 \text{ mol dm}^{-3} \text{ HCl}$  solution. Copper microdisk: A-  $6 \text{ }\mu\text{m}$  ; B-  $25 \text{ }\mu\text{m}$  in diameter. Staircase voltammetry:  $t = 2\text{s}$ ;  $\Delta E_s = 2 \text{ mV}$ .

FIGURE 1

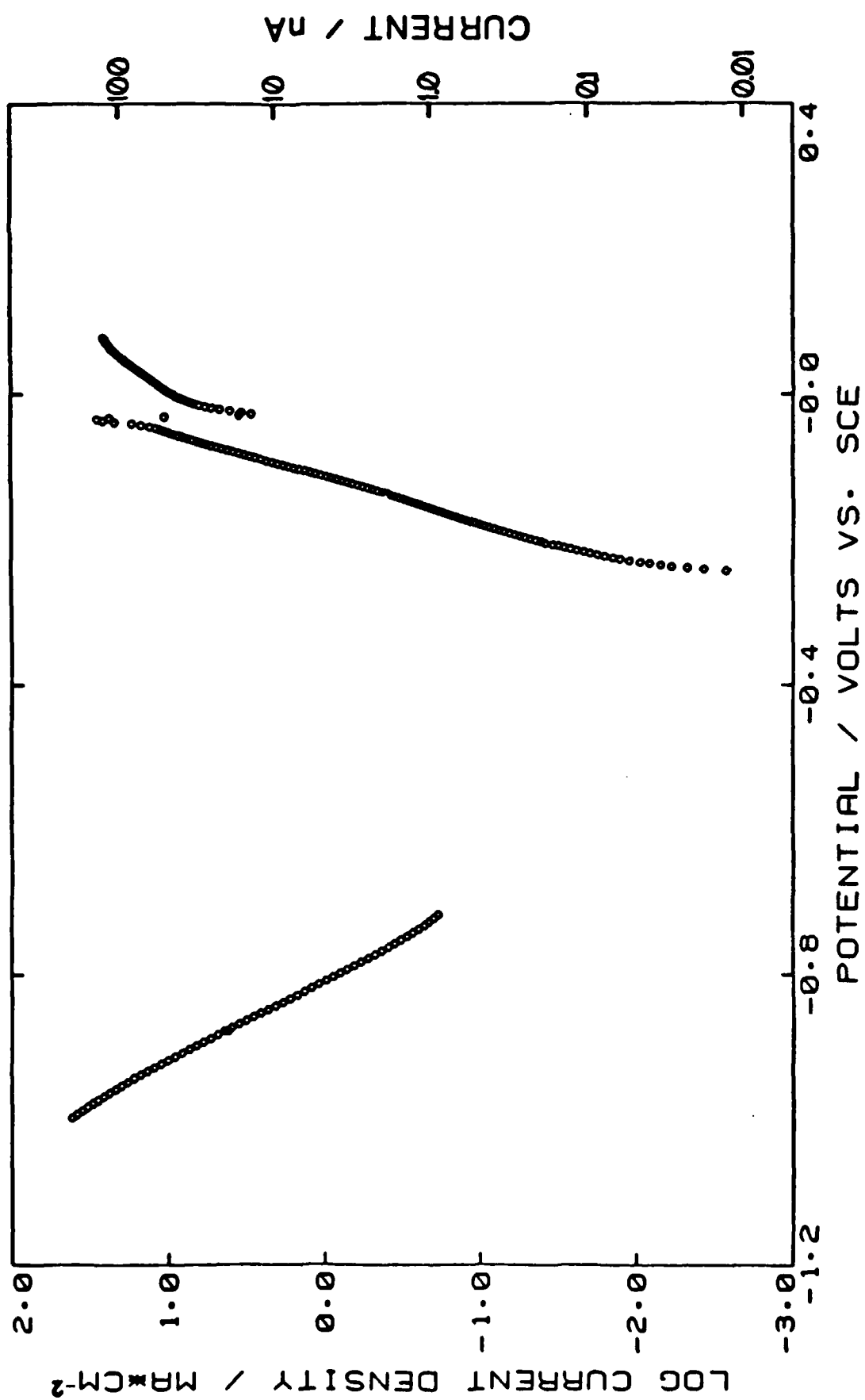


FIGURE 2

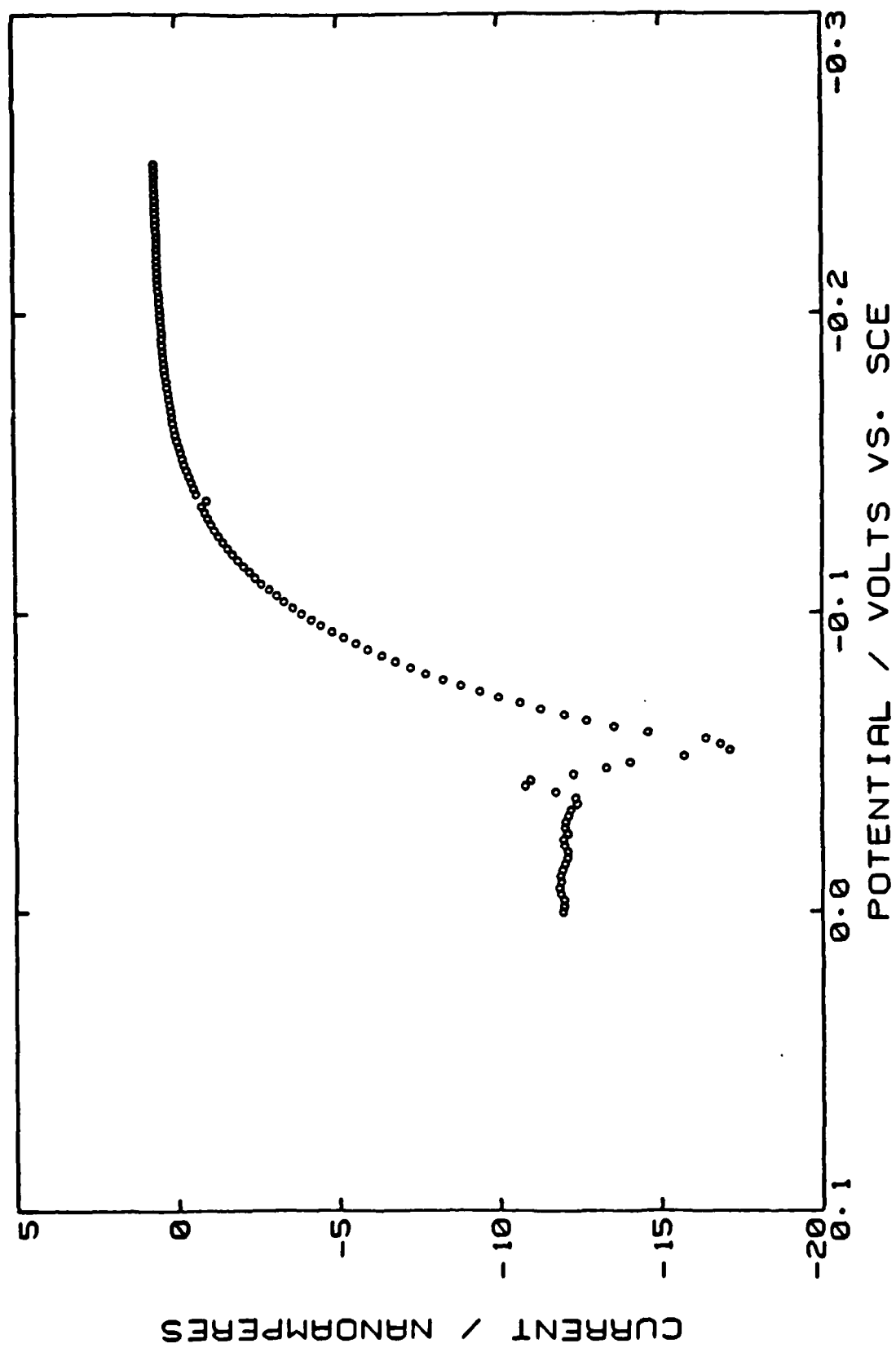


FIGURE 3

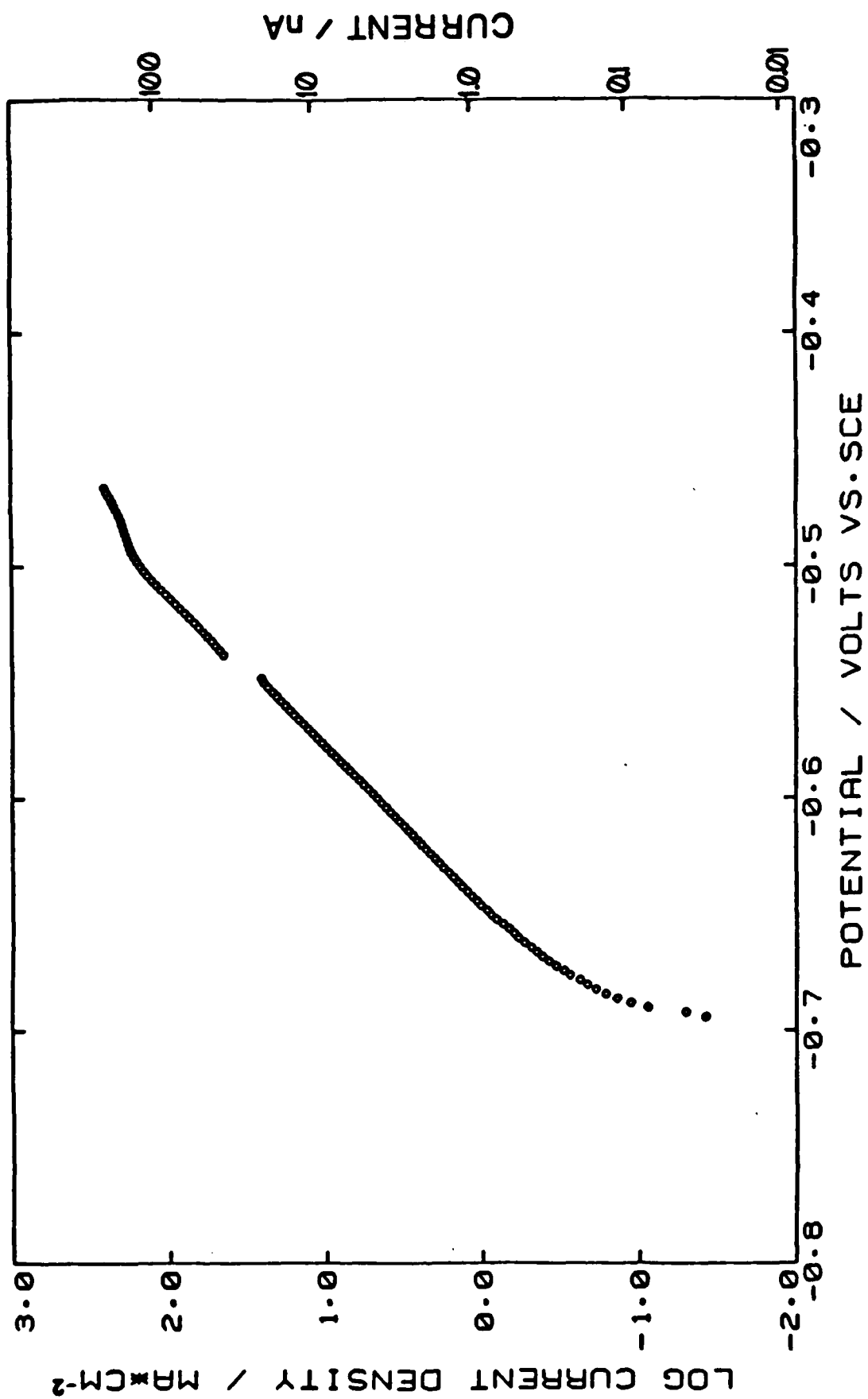


FIGURE 4

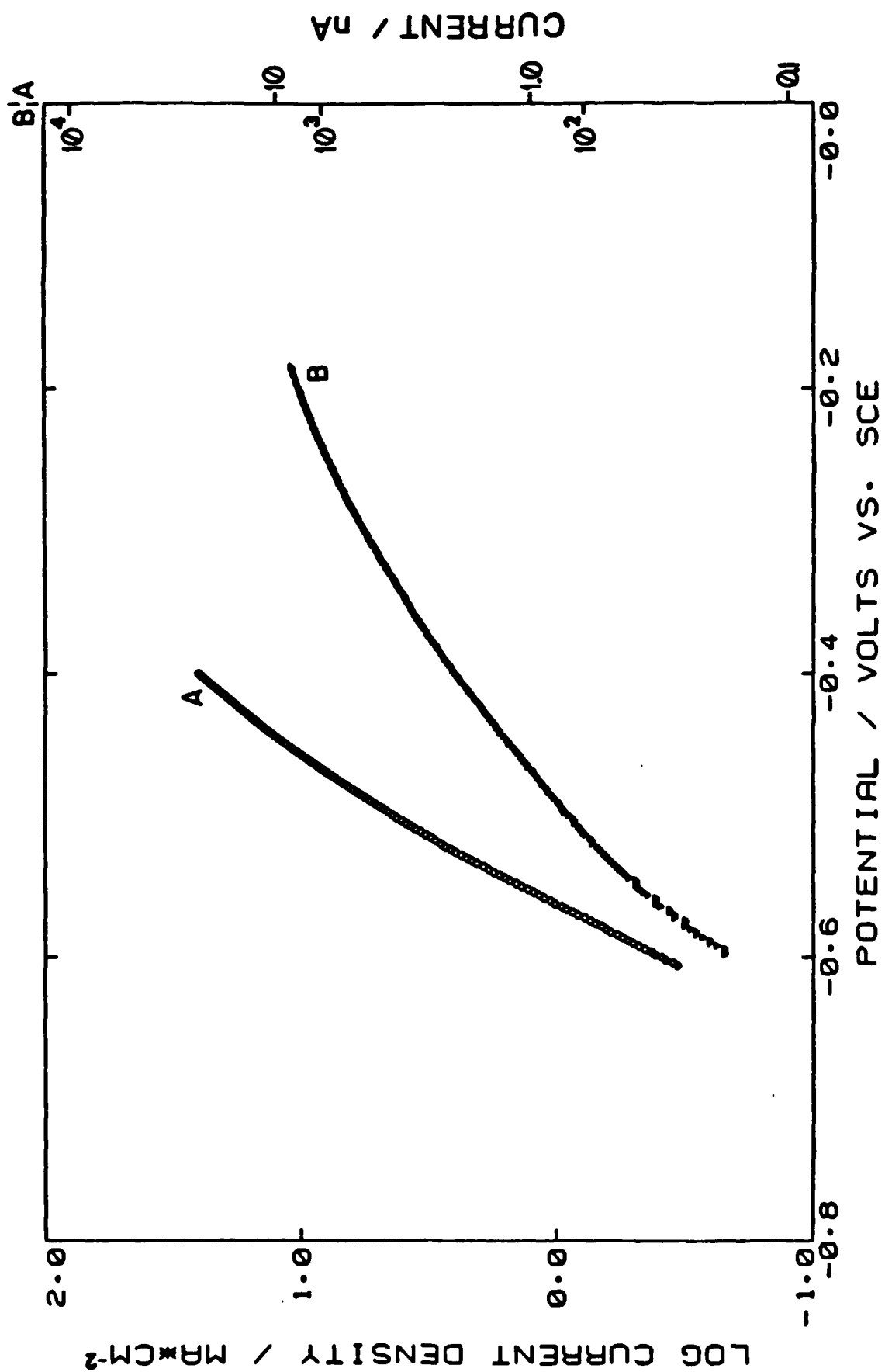




FIGURE 5

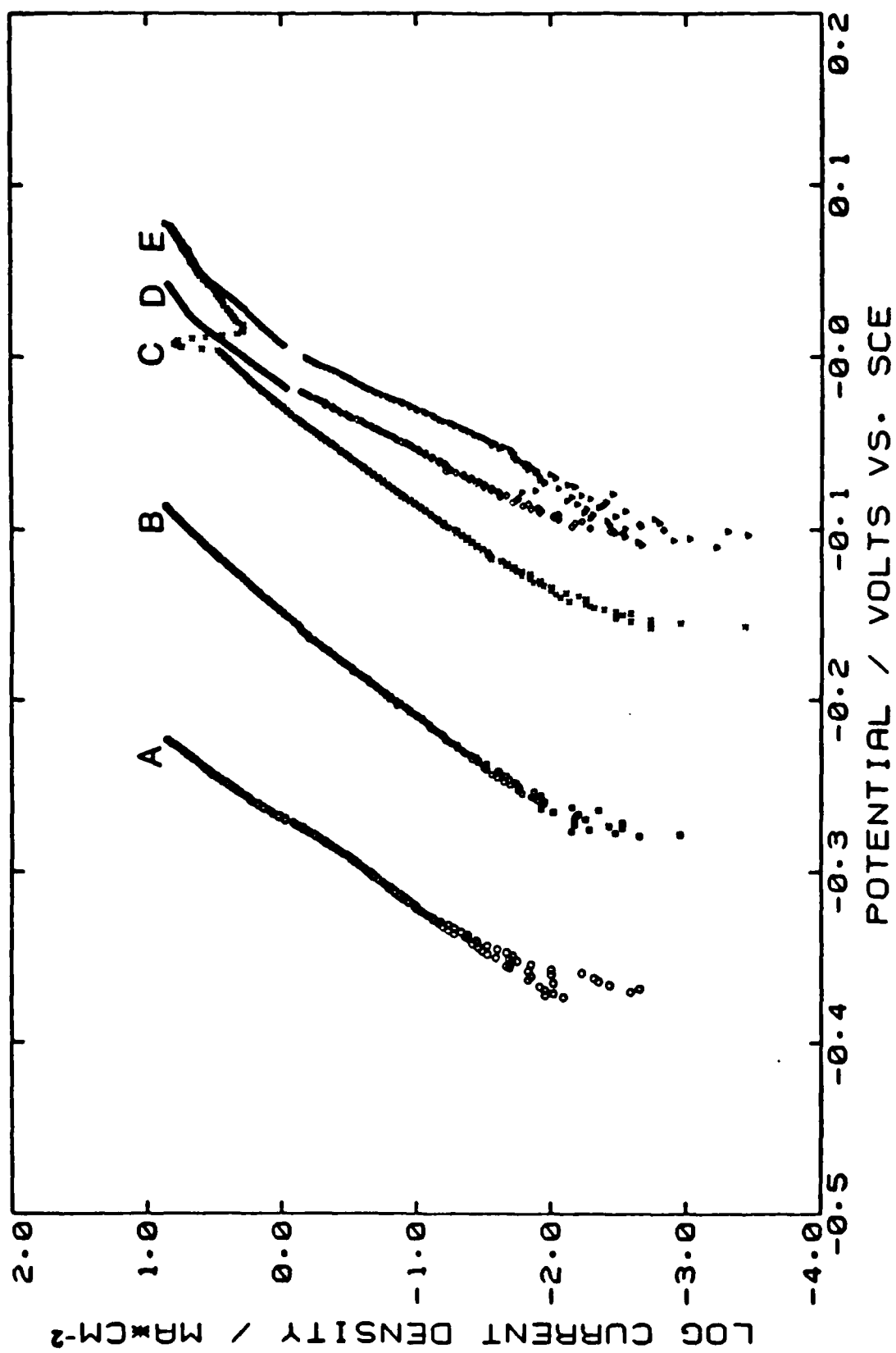
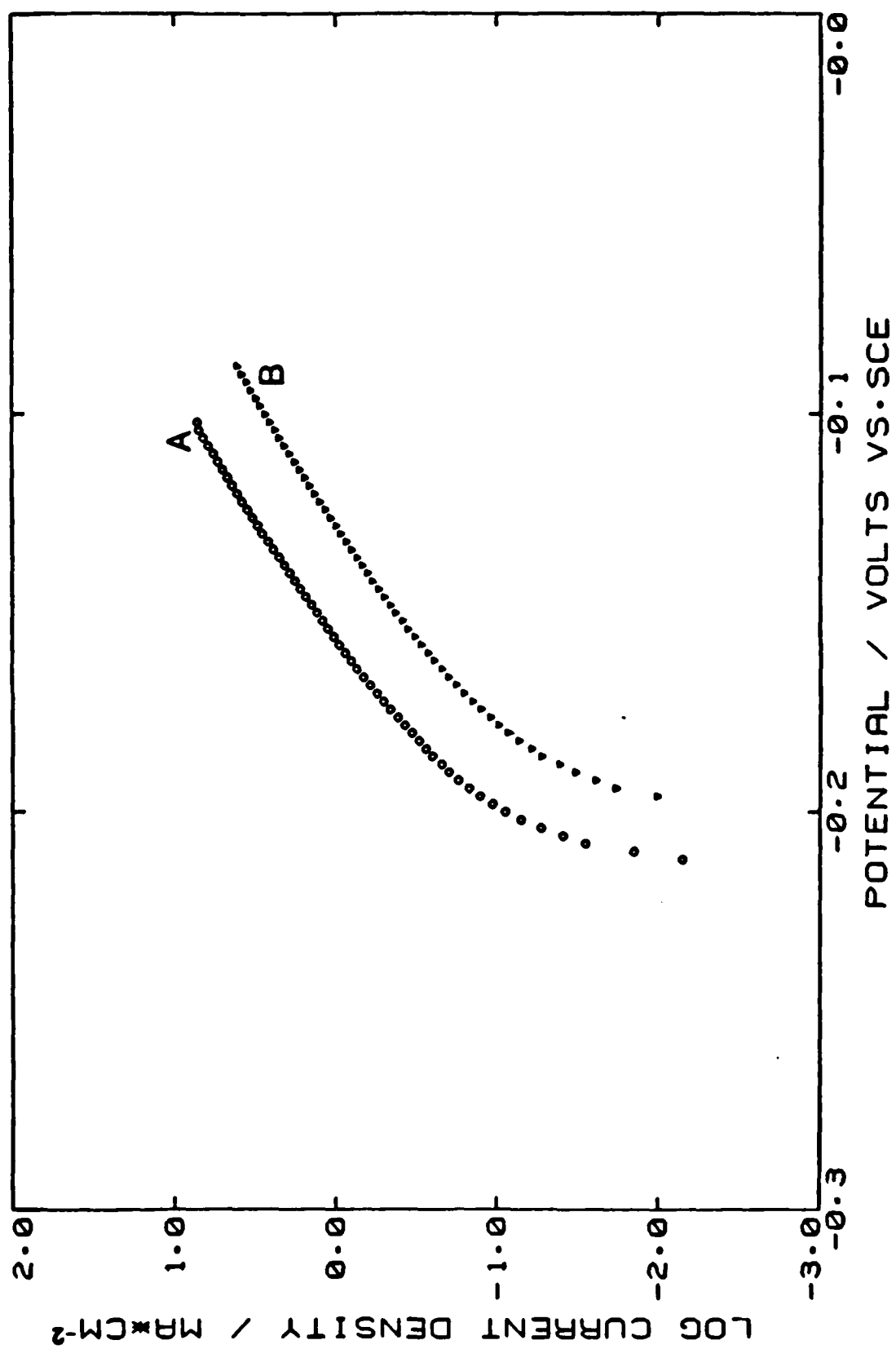


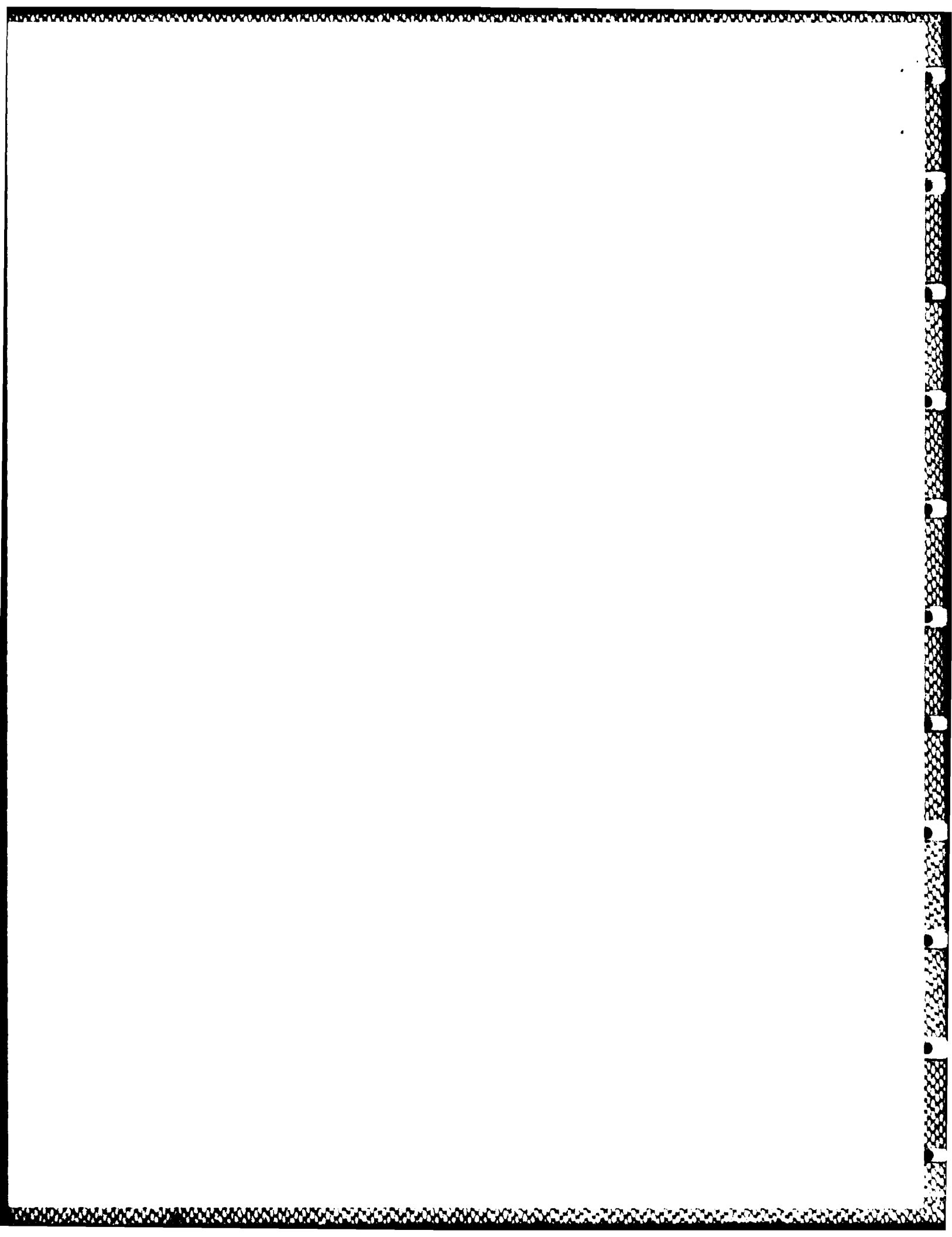
FIGURE 6



DL/1113/87/2

TECHNICAL REPORT DISTRIBUTION LIST, GEN

	<u>No. Copies</u>		<u>No. Copies</u>
✓ Office of Naval Research Attn: Code 1113 800 N. Quincy Street Arlington, Virginia 22217-5000	2	✓ Dr. David Young Code 334 NORDA NSTL, Mississippi 39529	1
✓ Dr. Bernard Douda Naval Weapons Support Center Code 50C Crane, Indiana 47522-5050	1	✓ Naval Weapons Center Attn: Dr. Ron Atkins Chemistry Division China Lake, California 93555	1
✓ Naval Civil Engineering Laboratory Attn: Dr. R. W. Drisko, Code L52 Port Hueneme, California 93401	1	✓ Scientific Advisor Commandant of the Marine Corps Code RD-1 Washington, D.C. 20380	1
✓ Defense Technical Information Center Building 5, Cameron Station Alexandria, Virginia 22314	12 high quality	✓ U.S. Army Research Office Attn: CRD-AA-IP P.O. Box 12211 Research Triangle Park, NC 27709	1
DTNSRDC ✓ Attn: Dr. H. Singerman Applied Chemistry Division Annapolis, Maryland 21401	1	✓ Mr. John Boyle Materials Branch Naval Ship Engineering Center Philadelphia, Pennsylvania 19112	1
✓ Dr. William Tolles Superintendent Chemistry Division, Code 6100 Naval Research Laboratory Washington, D.C. 20375-5000	1	✓ Naval Ocean Systems Center Attn: Dr. S. Yamamoto Marine Sciences Division San Diego, California 91232	1



ABSTRACTS DISTRIBUTION LIST, 359/627

Dr. Stanislaw Szpak  
Naval Ocean Systems Center  
Code 633, Bayside  
San Diego, California 95152

Dr. Gregory Farrington  
Department of Materials Science  
and Engineering  
University of Pennsylvania  
Philadelphia, Pennsylvania 19104

Dr. John Fontanella  
Department of Physics  
U.S. Naval Academy  
Annapolis, Maryland 21402-5062

Dr. Micha Tomkiewicz  
Department of Physics  
Brooklyn College  
Brooklyn, New York 11210

Dr. Lesser Blum  
Department of Physics  
University of Puerto Rico  
Rio Piedras, Puerto Rico 00931

Dr. Joseph Gordon, II  
IBM Corporation  
5600 Cottle Road  
San Jose, California 95193

Dr. Joel Harris  
Department of Chemistry  
University of Utah  
Salt Lake City, Utah 84112

Dr. J. O. Thomas  
University of Uppsala  
Institute of Chemistry  
Box 531 Baltimore, Maryland 21218  
S-751 21 Uppsala, Sweden

Dr. John Owen  
Department of Chemistry and  
Applied Chemistry  
University of Salford  
Salford M5 4WT UNITED KINGDOM

Dr. O. Stafsudd  
Department of Electrical Engineering  
University of California  
Los Angeles, California 90024

Dr. Boone Owens  
Department of Chemical Engineering  
and Materials Science  
University of Minnesota  
Minneapolis, Minnesota 55455

Dr. Johann A. Joebstl  
USA Mobility Equipment R&D Command  
DRDME-EC  
Fort Belvoir, Virginia 22060

Dr. Albert R. Landgrebe  
U.S. Department of Energy  
M.S. 6B025 Forrestal Building  
Washington, D.C. 20595

Dr. J. J. Brophy  
Department of Physics  
University of Utah  
Salt Lake City, Utah 84112

Dr. Charles Martin  
Department of Chemistry  
Texas A&M University  
College Station, Texas 77843

Dr. Milos Novotny  
Department of Chemistry  
Indiana University  
Bloomington, Indiana 47405

Dr. Mark A. McHugh  
Department of Chemical Engineering  
The Johns Hopkins University  
Baltimore, Maryland 21218

Dr. D. E. Irish  
Department of Chemistry  
University of Waterloo  
Waterloo, Ontario, Canada  
N2L 3G1

DL/1113/87/2

ABSTRACTS DISTRIBUTION LIST, 0518

Dr. R. A. Osteryoung  
Department of Chemistry  
State University of New York  
Buffalo, New York 14214

~~Dr. J. Osteryoung~~  
~~Department of Chemistry~~  
~~State University of New York~~  
~~Buffalo, New York 14214~~

Dr. B. R. Kowalski  
Department of Chemistry  
University of Washington  
Seattle, Washington 98105

Dr. A. Zirino  
Naval Undersea Center  
San Diego, California 92132

Dr. George H. Morrison  
Department of Chemistry  
Cornell University  
Ithaca, New York 14853

Dr. S. P. Perone  
Lawrence Livermore National  
Laboratory L-370  
P.O. Box 808  
Livermore, California 94550

Dr. M. B. Denton  
Department of Chemistry  
University of Arizona  
Tucson, Arizona 85721

Dr. M. Robertson  
Electrochemical Power Sources Division  
Code 305  
Naval Weapons Support Center  
Crane, Indiana 47522

Dr. G. M. Kieftje  
Department of Chemistry  
Indiana University  
Bloomington, Indiana 47401

Dr. Christie G. Enke  
Department of Chemistry  
Michigan State University  
East Lansing, Michigan 48824

Walter G. Cox, Code 3632  
Naval Underwater Systems Center  
Building 148  
Newport, Rhode Island 02840

Professor Isiah M. Warner  
Department of Chemistry  
Emory University  
Atlanta, Georgia 30322

Dr. Kent Eisentraut  
Air Force Materials Laboratory  
Wright-Patterson AFB, Ohio 45433

Dr. John Eyler  
Department of Chemistry  
University of Florida  
Gainesville, Florida 32611

Dr. B. E. Douda  
Chemical Sciences Branch  
Code 50 C  
Naval Weapons Support Center  
Crane, Indiana 47322

Professor J. Janata  
Department of Bioengineering  
University of Utah  
Salt Lake City, Utah 84112

Dr. J. DeCorpo  
NAVSEA  
Code 05 R32  
Washington, D.C. 20362

Dr. Ron Flemming  
B 108 Reactor  
National Bureau of Standards  
Washington, D.C. 20234

Dr. Frank Herr  
Office of Naval Research  
Code 422CB  
800 N. Quincy Street  
Arlington, Virginia 22217

Dr. Marvin Wilkerson  
Naval Weapons Support Center  
Code 30511  
Crane, Indiana 47522

ABSTRACTS DISTRIBUTION LIST, 359/627

Dr. Manfred Breiter  
Institut für Technische Elektrochemie  
Technischen Universität Wien  
9 Getreidemarkt, 1160 Wien  
AUSTRIA

Dr. E. Yeager  
Department of Chemistry  
Case Western Reserve University  
Cleveland, Ohio 44106

Dr. R. Sutula  
The Electrochemistry Branch  
Naval Surface Weapons Center  
Silver Spring, Maryland 20910

Dr. R. A. Marcus  
Department of Chemistry  
California Institute of Technology  
Pasadena, California 91125

Dr. J. J. Auborn  
AT&T Bell Laboratories  
600 Mountain Avenue  
Murray Hill, New Jersey 07974

Dr. M. S. Wrighton  
Chemistry Department  
Massachusetts Institute  
of Technology  
Cambridge, Massachusetts 02139

Dr. B. Stanley Pons  
Department of Chemistry  
University of Utah  
Salt Lake City, Utah 84112

Dr. Bernard Spielvogel  
U.S. Army Research Office  
P.O. Box 12211  
Research Triangle Park, NC 27709

Dr. Mel Miles  
Code 3852  
Naval Weapons Center  
China Lake, California 93555

Dr. P. P. Schmidt  
Department of Chemistry  
Oakland University  
Rochester, Michigan 48063

Dr. Roger Belt  
Litton Industries Inc.  
Airtron Division  
Morris Plains, NJ 07950

Dr. Ulrich Stimming  
Department of Chemical Engineering  
Columbia University  
New York, NY 10027

Dr. Royce W. Murray  
Department of Chemistry  
University of North Carolina  
Chapel Hill, North Carolina 27514

Dr. Michael J. Weaver  
Department of Chemistry  
Purdue University  
West Lafayette, Indiana 47907

Dr. R. David Rauh  
EIC Laboratories, Inc.  
Norwood, Massachusetts 02062

Dr. Edward M. Eyring  
Department of Chemistry  
University of Utah  
Salt Lake City, UT 84112

Dr. M. M. Nicholson  
Electronics Research Center  
Rockwell International  
3370 Miraloma Avenue  
Anaheim, California

Dr. Nathan Lewis  
Department of Chemistry  
Stanford University  
Stanford, California 94305

Dr. Hector D. Abruna  
Department of Chemistry  
Cornell University  
Ithaca, New York 14853

Dr. A. B. P. Lever  
Chemistry Department  
York University  
Downsview, Ontario M3J 1P3

ABSTRACTS DISTRIBUTION LIST, 051B

DL/1113/87/2

Dr. Alice Harper  
Code 3851  
Naval Weapons Center  
China Lake, California 93555

Dr. J. Wyatt  
Naval Research Laboratory  
Code 6110  
Washington, D.C. 20375-5000

Dr. J. MacDonald  
Code 6110  
Naval Research Laboratory  
Washington, D.C. 20375-5000

Dr. Andrew T. Zander P1207  
Perkin-Elmer Corporation  
901 Ethan Allen Highway/MS905  
Ridgefield, Connecticut 06877

Dr. A. B. Ellis  
Department of Chemistry  
University of Wisconsin  
Madison, Wisconsin 53706

Dr. Robert W. Shaw  
U.S. Army Research Office  
Box 12211  
Research Triangle Park, NC 27709

Dr. John Hoffsommer  
Naval Surface Weapons Center  
Building 30 Room 208  
Silver Spring, Maryland 20910



ABSTRACTS DISTRIBUTION LIST, 359/627

Dr. Martin Fleischmann  
Department of Chemistry  
University of Southampton  
Southampton SO9 5H UNITED KINGDOM

Dr. John Wilkes  
Department of the Air Force  
United States Air Force Academy  
Colorado Springs, Colorado 80840-6528

Dr. R. A. Osteryoung  
Department of Chemistry  
State University of New York  
Buffalo, New York 14214

Dr. Janet Osteryoung  
Department of Chemistry  
State University of New York  
Buffalo, New York 14214

Dr. A. J. Bard  
Department of Chemistry  
University of Texas  
Austin, Texas 78712

Dr. Steven Greenbaum  
Department of Physics and Astronomy  
Hunter College  
695 Park Avenue  
New York, New York 10021

Dr. Donald Sandstrom  
Boeing Aerospace Co.  
P.O. Box 3999  
Seattle, Washington 98124

Mr. James R. Moden  
Naval Underwater Systems Center  
Code 3632  
Newport, Rhode Island 02840

Dr. D. Rolison  
Naval Research Laboratory  
Code 6171  
Washington, D.C. 20375-5000

Dr. D. F. Shriver  
Department of Chemistry  
Northwestern University  
Evanston, Illinois 60201

Dr. Alan Bewick  
Department of Chemistry  
The University of Southampton  
Southampton, SO9 5NH UNITED KINGDOM

Dr. Edward Fletcher  
Department of Mechanical Engineering  
University of Minnesota  
Minneapolis, Minnesota 55455

Dr. Bruce Dunn  
Department of Engineering &  
Applied Science  
University of California  
Los Angeles, California 90024

Dr. Elton Cairns  
Energy & Environment Division  
Lawrence Berkeley Laboratory  
University of California  
Berkeley, California 94720

Dr. Richard Pollard  
Department of Chemical Engineering  
University of Houston  
Houston, Texas 77004

Dr. M. Philpott  
IBM Research Division  
Mail Stop K 33/801  
San Jose, California 95130-6099

Dr. Martha Greenblatt  
Department of Chemistry, P.O. Box 939  
Rutgers University  
Piscataway, New Jersey 08855-0939

Dr. Anthony Sammells  
Eltron Research Inc.  
4260 Westbrook Drive, Suite 111  
Aurora, Illinois 60505

Dr. C. A. Angell  
Department of Chemistry  
Purdue University  
West Lafayette, Indiana 47907

Dr. Thomas Davis  
Polymers Division  
National Bureau of Standards  
Gaithersburg, Maryland 20899

DL/1113/87/2

ABSTRACTS DISTRIBUTION LIST, 359/627

Dr. Henry S. White  
Department of Chemical Engineering  
and Materials Science  
151 Amundson Hall  
421 Washington Avenue, S.E.  
Minneapolis, Minnesota 55455

Dr. Daniel A. Buttry  
Department of Chemistry  
University of Wyoming  
Laramie, Wyoming 82071

Dr. W. R. Fawcett  
Department of Chemistry  
University of California  
Davis, California 95616

Dr. Peter M. Blonsky  
Eveready Battery Company, Inc.  
25225 Detroit Road, P.O. Box 45035  
Westlake, Ohio 44145